

Compton scattering study of the silicon clathrate Ba₈Si₄₆: Experiment and theory

M. Itou* and Y. Sakurai

Japan Synchrotron Radiation Research Institute (JASRI), SPring-8, 1-1-1 Kouto, Mikazuki, Sayo, Hyogo 679-5198, Japan

M. Usuda

Synchrotron Radiation Research Center, Japan Atomic Energy Research Institute (JAERI), 1-1-1 Kouto, Mikazuki, Sayo, Hyogo 679-5148, Japan

C. Cros

Institut de Chimie de la Matière Condensée de Bordeaux, Université Bordeaux I, 33608 Pessac, France

H. Fukuoka and S. Yamanaka

Department of Applied Chemistry, Faculty of Engineering, Hiroshima University, Higashi-Hiroshima 739-8527, Japan

(Received 29 June 2004; revised manuscript received 12 November 2004; published 24 March 2005)

The Compton profile of the Ba doped silicon clathrate (Ba₈Si₄₆) has been studied using the high-resolution Compton scattering technique. The Compton profile is sensitive to the change of wave functions, and the good agreement between experiment and theory validates a theoretical prediction. A difference Compton profile between the Ba doped and nondoped clathrates (Si₁₃₆) has been experimentally obtained and compared with that of a first-principles band structure calculation. The experiment and calculation show excellent agreement with respect to the overall shape in the profile. Analyses of partial density of the states (DOS) predict that, by doping Ba atoms into the Si cages, Ba 6*s* electrons are transferred into Ba 5*d* orbitals that are strongly hybridized with Si 3*p* orbitals. The hybridized states form a sharp peak of the DOS in close vicinity of the Fermi level, which plays an important role for the occurrence of superconductivity in Ba₈Si₄₆.

DOI: 10.1103/PhysRevB.71.125125

PACS number(s): 78.70.Ck, 71.15.Ap, 74.25.Jb, 74.70.Wz

I. INTRODUCTION

Barium-doped type-I silicon clathrates have attracted considerable attention since the discovery of superconductivity in Na₂Ba₆Si₄₆.^{1,2} Although the transition temperature, T_c , is about 4 K, the silicon clathrates have been intensively studied in connection with the electron-doped C₆₀ compounds with a value of T_c higher than 30 K.³ Later, the binary compound Ba_{8- δ} Si₄₆ with $T_c=8$ K has been synthesized under a high pressure and high temperature condition.⁴ Recently, it has been reported that superconductivity is expected at T_c higher than 10 K at the stoichiometric composition Ba₈Si₄₆.⁵ In parallel with the efforts for synthesizing higher quality samples, the mechanism of superconductivity has been investigated. A phonon-mediated Bardeen-Cooper-Schrieffer (BCS) scenario has been proposed in connection with the superconductivity in doped fullerenes.⁶ In the BCS mechanism, T_c depends on two terms: one is the density of states (DOS) at the Fermi level (E_F) and the other is the electron-phonon coupling factor. The type-I silicon clathrate has a Si-*sp*³ covalent bonding network, which is composed of fullerene-like Si₂₀ dodecahedral and Si₂₄ tetrakaidecahedral cages.^{7,8} The high rigidity of the network causes a high Debye temperature, which favors the occurrence of superconductivity in terms of the electron-phonon coupling. Recent experiments⁹⁻¹¹ have pointed out the importance of the vibrational coupling between the guest atoms and the host Si-*sp*³ network. In addition, the observation of Si isotope effects¹² and the analyses of the pressure dependence of T_c (Ref. 13) provide pieces of evidence that the BCS mecha-

nism accounts for superconductivity in Ba₈Si₄₆. Regarding the electronic structure, first-principles calculations^{14,15} have predicted high DOS at E_F in Na₂Ba₆Si₄₆ and Ba₈Si₄₆. The high DOS at E_F is caused by the strong hybridization of Ba 5*d* orbitals with Si₄₆ conduction bands and is presumably essential to play another key role for the occurrence of superconductivity in the Ba-doped silicon clathrates. On the experimental side, however, there have been only a few photoemission studies^{16,17} to investigate the electronic structure, and thus the validity of the calculations is still inconclusive in connection with the predicted high DOS at E_F .

The aim of this study is to investigate the electronic structure of Ba₈Si₄₆ in terms of electron momentum density. In this paper, we report experimental and theoretical Compton profiles in Ba₈Si₄₆ and its related compounds. The Compton profiles have been measured by the high-resolution Compton scattering technique, and the theoretical ones have been computed from the wave functions obtained by first-principles band-structure calculations.

The Compton profile, $J(p_z)$, is defined as a one-dimensional projection of the ground-state electron momentum density, $n(\mathbf{p})$,^{18,19}

$$J(p_z) = \iint n(\mathbf{p}) dp_x dp_y, \quad (1)$$

where p_x , p_y , and p_z are the Cartesian momentum components, and the z axis is parallel to the scattering vector. In an independent-particle model, the momentum density is given by

$$n(\mathbf{p}) = (2\pi)^{-3} \sum_i \left| \int \psi_i(\mathbf{r}) \exp(i\mathbf{p} \cdot \mathbf{r}) d\mathbf{r} \right|^2, \quad (2)$$

where $\psi_i(\mathbf{r})$ is an electron wave function.²⁰ The summation in Eq. (2) extends over all the occupied states. The area under the Compton profile gives the total number of electrons N ,

$$\int_{-\infty}^{\infty} J(p_z) dp_z = N. \quad (3)$$

The Compton profile is sensitive to the change of wave functions, and its measurements provide a testing ground for theoretical wave functions.^{18,21} The good agreement between experiment and theory validates the quality of discussions on the electronic structure based on the theoretical predictions.

Unlike conventional photoemission spectroscopy, Compton scattering is very bulk sensitive, and unlike the de Haas–van Alphen and angular correlation of positron annihilation radiation measurements it is insensitive to defects and impurities in a sample. These notable features provide complementary information on the electronic structure of $\text{Ba}_8\text{Si}_{46}$.

II. EXPERIMENT

A sample of $\text{Ba}_{8-\delta}\text{Si}_{46}$ was synthesized by a high pressure technique.⁴ Samples prepared by the same procedure show superconductivity below $T_c=8$ K, and thus the present sample might have Ba deficiency of $\delta \approx 0.5$.⁵ In order to obtain the difference profile between $\text{Ba}_8\text{Si}_{46}$ and Si_{46} , a reference sample Si_{46} should be used. However, Si_{46} with no metal doping has not yet been synthesized. As a good substitute for Si_{46} , the type-II silicon clathrate Si_{136} was prepared by thermal decomposition of a solid solution of NaSi Zintl phase under high vacuum at 340–420 °C.²² The Si_{136} clathrate consists of face shared Si_{20} and Si_{28} polyhedra, each silicon being tetrahedrally coordinated in a manner very similar to that of the Si_{46} clathrate, which consists of face shared Si_{20} and Si_{24} polyhedra. The residual amount of Na in the prepared $\text{Na}_x\text{Si}_{136}$ was estimated to be as small as $0.5 < x < 1$, and homogeneously doped into the Si_{28} cages of Si_{136} . The sample is hereafter called Si_{136} . The powder samples were packed into the sample cases with a thickness of 2 mm. The packing density was about 50%. A cubic-diamond Si (*cd*-Si) sample was also measured for comparison.

The Compton scattering experiment was carried out using a Cauchois-type x-ray spectrometer which was installed at BL08W, SPring-8.^{23–25} The energy of the incident x rays was 116 keV and the scattering angle was 165°. The experimental momentum resolution was 0.16 atomic units (a.u.). The Compton profile measurements were performed at room temperature. The data processing to deduce the Compton profile from the raw energy spectrum consists of the following procedures: background subtraction; and energy-dependent corrections for the Compton scattering cross section, the absorption of incident and scattered x rays in the sample, the efficiency of the analyzer and the detector. A valence-electron Compton profile is obtained by subtracting the the-

oretical core-electron profile²⁶ from the experimental total-electron Compton profile. Here, $(1s)^2-(4d)^{10}(5s)^2(5p)^6$ for Ba and $(1s)^2(2s)^2(2p)^6$ for Si are treated as the core electrons. The profiles were folded to improve the effective statistics after confirming that they appeared symmetric about $p_z=0$ within error bars. In the data-processing, multiple scattering corrections were not employed since the effect on the difference profiles are negligible. Simulations with a Monte Carlo program²⁷ showed that the double-Compton-scattering events are about 1.7% of the sum of the single- and double-scattered events for the samples. The simulated energy profile of the double-scattered events are almost identical among them, and thus the multiple-scattering events are almost canceled out in the difference profiles.

III. CALCULATION

Theoretical Compton profiles of $\text{Ba}_8\text{Si}_{46}$ and Si_{46} were calculated from the wave functions obtained by the full-potential linearized augmented-plane-wave (FLAPW) method^{28,29} within the local-density approximation (LDA). The local exchange-correlation functional of Vosko, Wilk, and Nusair³⁰ was employed. The angular momentum in the spherical-wave expansion was truncated at $l_{\text{max}}=6$ and $l_{\text{max}}=7$ for the potential and wave function, respectively. The cutoff of the plane wave for the wave function was 12 Ry. We took 64 k points in the first Brillouin zone for both crystals. In order to obtain the Compton profiles, the momentum density $n(\mathbf{p})$ was calculated on a mesh up to $|\mathbf{p}|=5$ a.u., where $\mathbf{p}=\mathbf{k}+\mathbf{G}$ and \mathbf{G} is a reciprocal lattice vector. The two-dimensional integration involved in the evaluation of the Compton profile [see Eq. (1)] were carried out by utilizing a spherical harmonics expansion method. A theoretical Compton profile of *cd*-Si was also computed for comparison.

IV. RESULTS AND DISCUSSION

The experimental and theoretical results are shown in Fig. 1. The open circles show the experimental difference Compton profile between $\text{Ba}_{8-\delta}\text{Si}_{46}$ and Si_{136} , and the solid line shows the theoretical one between $\text{Ba}_8\text{Si}_{46}$ and Si_{46} . The area under the experimental Compton profile of Si_{136} is normalized to the value for Si_{46} , assuming that the shape of both profiles are close to each other. The validity of this assumption will be discussed in the next paragraph. Under the present normalization, the Na content of $x=1$ for $\text{Na}_x\text{Si}_{136}$ causes the error in $\Delta J_{\text{val}}(p_z)$ of 0.3 at $p_z=0$ and the Ba deficiency of $\delta=0.5$ for $\text{Ba}_{8-\delta}\text{Si}_{46}$ makes the error of 2.2. These errors are comparable in size to the statistical error bars. The experiment and theory reveal an excellent agreement on the overall shape of the profile. The open triangles show the experimental difference Compton profile between *cd*-Si and Si_{136} , where the areas under both Compton profiles are normalized to the value for Si_{46} . The profile is almost flat, indicating that the Compton profiles in both materials are close to each other. The broken line is the theoretical difference Compton profile between *cd*-Si and Si_{46} , predicting little difference between them.

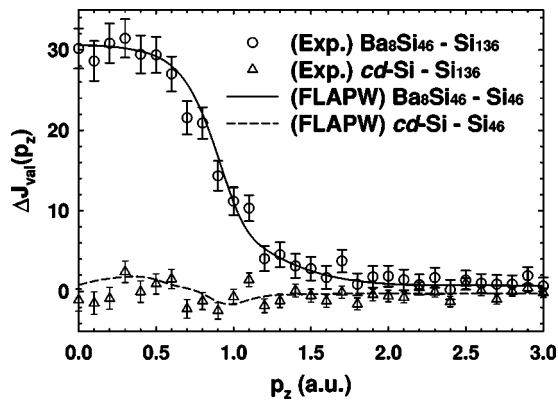


FIG. 1. Experimental and theoretical difference Compton profiles: The open circles and open triangles show experimental difference Compton profiles between $\text{Ba}_{8-9}\text{Si}_{46}$ and Si_{136} and between $cd\text{-Si}$ and Si_{136} . The solid line and broken line are theoretical difference Compton profiles between $\text{Ba}_8\text{Si}_{46}$ and Si_{46} and between $cd\text{-Si}$ and Si_{46} . The areas under the Si_{136} and $cd\text{-Si}$ Compton profiles for the experiment and theory are normalized to that of Si_{46} .

The present experiment and calculation suggest that the directionally-averaged momentum density distributions between $cd\text{-Si}$, Si_{46} , and Si_{136} are very close to each other. This is consistent with the fact that all the Si atoms are tetrahedrally coordinated and are connected with sp^3 covalent bonding in these materials. The momentum density of electrons in bonds was theoretically studied by Coulson *et al.*^{31,32} and by Weyrich *et al.*³³ They showed that the presence of bonding gives rise to a periodic oscillation and an angular dependence in the momentum density. Directional averaging, due to powder samples, conceals the angular dependence of the Si network from observation, and thus make only the bond-length aspect of Si sp^3 covalent bonding remained. The period in the oscillation depends on the interatomic distance between atoms sharing the bond. In the present case, the bond-lengths for the Si_{46} and Si_{136} clathrates (2.37 Å) are almost same to that of $cd\text{-Si}$ (2.35 Å), leading to almost the same shapes in the Compton profile among $cd\text{-Si}$, Si_{46} , and Si_{136} . Such a small difference is consistent with the results of calculations

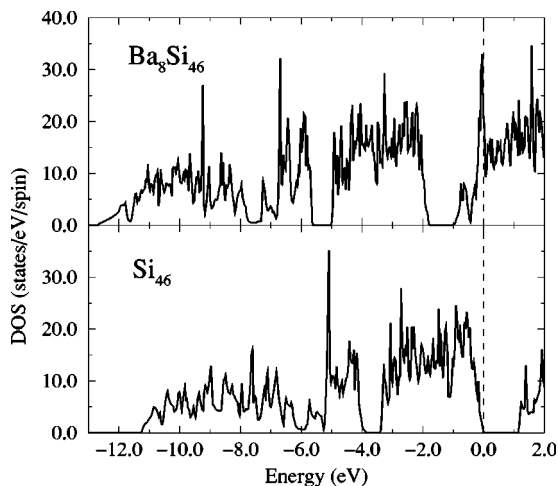


FIG. 2. Total DOS of $\text{Ba}_8\text{Si}_{46}$ and Si_{46} . Energy is measured from the Fermi level E_F .

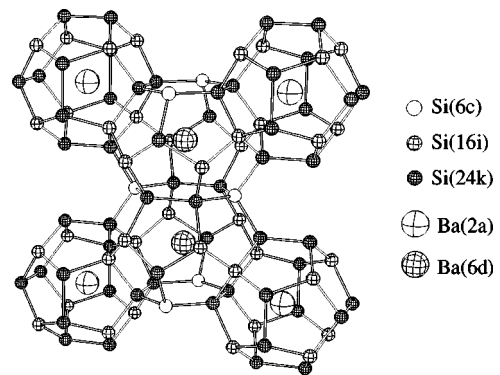


FIG. 3. Structure of Si_{20} and Si_{24} cages and the Ba atoms in $\text{Ba}_8\text{Si}_{46}$.

on the energetics and band structures by Adams *et al.*³⁴ They have shown that the total energy difference between the Si clathrates and the $cd\text{-Si}$ is 0.07 eV, that is three times smaller than that between the $\beta\text{-tin}$ and cd phases of Si.

As seen in Fig. 1, the calculated profiles reproduce well the experimental profiles, demonstrating the usefulness of the band-structure calculations. Now we discuss in detail the band structures. Figure 2 shows the total DOS of $\text{Ba}_8\text{Si}_{46}$ and Si_{46} . The obtained results are in good agreement with the previously reported results.^{14,15} In Si_{46} the fundamental gap is 1.15 eV, which is larger than the $cd\text{-Si}$ gap of 0.48 eV, and there is another band gap in the valence-band region from -3.8 to -3.4 eV. In $\text{Ba}_8\text{Si}_{46}$ there is a strong DOS peak in close vicinity of E_F .

The strong DOS peak near E_F presumably comes from the hybridized band of the Ba $5d$ states with the Si_{46} conduction bands.^{14,15} In order to see this point clearly, we present the projected DOS onto the atomic orbitals at each site. There are three Si sites: (6c), (16i), and (24k) sites; and two Ba sites: (2a) and (6d) sites. The Ba (2a) site is at the center of the Si_{20} cage and the Ba (6d) site is at the center of the Si_{24}

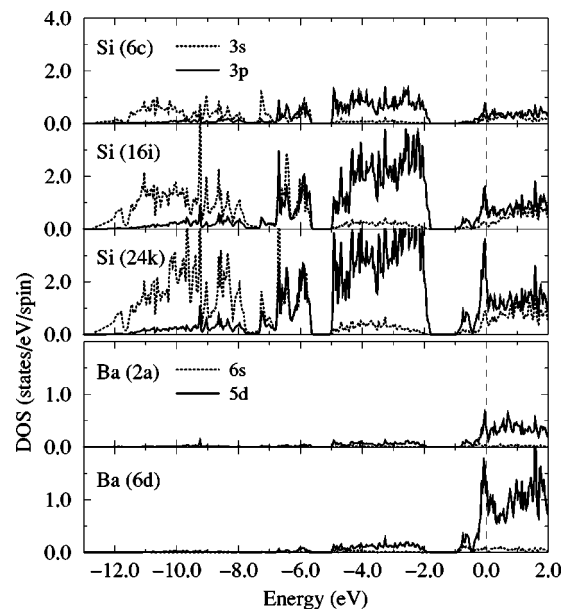


FIG. 4. Partial DOS of $\text{Ba}_8\text{Si}_{46}$. Energy is measured from the top of the valence band.

cage (see Fig. 3). Figure 4 displays the partial DOS for the Si 3s and 3p states and for the Ba 6s and 5d states at each site. It is found that the valence bands from -12.7 to -1.9 eV are composed of three parts: the Si s-like states in the lower energy side, the Si sp hybridized states in the middle, and the Si p-like states in the higher energy side. The band edge of the Ba 5d states are slightly lower than E_F and much hybridized with the Si p-like conduction bands, forming the strong DOS peak in close vicinity of E_F . The contribution of the Ba 6s states to the DOS near E_F is quite small. This indicates that most of the 6s electrons of doped Ba atoms are transferred into the Ba 5d states to form the strong DOS peak near E_F . The electron transfer from the Ba 6s to 5d states has been also found in other Ba compounds.³⁵ Such a high DOS near E_F has been also predicted in A_3C_{60} ($A=K, Rb$, etc.) fullerene compounds, and plays an important role in the occurrence of superconductivity.⁶ On the other hand, a strong vibrational coupling between the Ba atoms and the Si cages has been suggested in the Ba_8Si_{46} compounds.⁹⁻¹¹ The high DOS near E_F and the vibrational coupling between Ba atoms and Si cages are responsible for the superconductivity in Ba_8Si_{46} .

In summary, we have measured the Compton profiles of Ba_8Si_{46} , Si_{136} , and *cd*-Si powder samples by a high-resolution Compton scattering technique. In parallel with the

experiments, FLAPW-LDA band-structure calculations on Ba_8Si_{46} , Si_{46} , and *cd*-Si have been carried out and the theoretical Compton profiles have been obtained. The experiment and calculation show a good level of accord in the overall shapes and the height of the difference Compton profiles between the Ba doped clathrate and the nondoped clathrate. Analyses of partial DOS reveals that the Ba 5d states are hybridized with the Si 3p states, forming the strong peak in close vicinity of the Fermi level. The Ba 6s orbitals are nearly empty. This leads to a conclusion that the Ba 6s electrons are transferred into the Ba 5d orbitals to form a strong hybridization with Si 3p orbitals. The hybridized states cause a high DOS at the Fermi level, which favors superconductivity in Ba_8Si_{46} .

ACKNOWLEDGMENTS

The computational code of FLAPW calculation including Compton profile calculation was developed by Kodama, Hamada, and Yanase. This study was supported in part by Grant-in-Aid for Scientific Research (A) (No.16205027) and the COE Research (No.13CE2002) of the Ministry of Education, Culture, Sports, Science and Technology of Japan. The Compton scattering experiment was performed with the approval of JASRI (Proposal No. 2002A0576-ND3-np).

*Electronic address: mito@spring8.or.jp

¹S. Yamanaka, H. Horie, H. Nakano, and M. Ishikawa, *Fullerene Sci. Technol.* **3**, 21 (1995).
²H. Kawaji *et al.*, *Phys. Rev. Lett.* **74**, 1427 (1995).
³O. Gunnarsson, *Rev. Mod. Phys.* **69**, 575 (1994).
⁴S. Yamanaka *et al.*, *Inorg. Chem.* **39**, 56 (2000).
⁵H. Fukuoka, J. Kiyoto, and S. Yamanaka, *Inorg. Chem.* **42**, 2933 (2003).
⁶R. Fleming, A. Ramirez, M. Rosseinsky, D. Murphy, R. Haddon, S. M. Zahurak, and A. Makhija, *Nature (London)* **352**, 787 (1991).
⁷J. S. Kasper, P. Hagemuller, M. Pouchard, and C. Cros, *Science* **150**, 1713 (1965).
⁸C. Cros, M. Pouchard, and P. Hagemuller, *J. Solid State Chem.* **2**, 570 (1970).
⁹P. Mélinon, P. Kéghélian, A. Perez, B. Champagnon, Y. Guyot, L. Saviot, E. Reny, C. Cros, M. Pouchard, and A. J. Dianoux, *Phys. Rev. B* **59**, 10099 (1999).
¹⁰E. Reny *et al.*, *Phys. Rev. B* **66**, 014532 (2002).
¹¹T. Kume, H. Fukuoka, T. Koda, S. Sasaki, H. Shimizu, and S. Yamanaka, *Phys. Rev. Lett.* **90**, 155503 (2003).
¹²K. Tanigaki, T. Shimizu, K. M. Itoh, J. Teraoka, Y. Moritomo, and S. Yamanaka, *Nat. Mater.* **2**, 653 (2003).
¹³D. Connétable *et al.*, *Phys. Rev. Lett.* **91**, 247001 (2003).
¹⁴S. Saito and A. Oshiyama, *Phys. Rev. B* **51**, R2628 (1995).
¹⁵K. Moriguchi, M. Yonemura, A. Shintani, and S. Yamanaka, *Phys. Rev. B* **61**, 9859 (2000).
¹⁶P. Mélinon, P. Kéghélian, X. Blase, J. LeBrusq, A. Perez, E. Reny, C. Cros, and M. Pouchard, *Phys. Rev. B* **58**, 12590 (1998).
¹⁷T. Yokoya, A. Fukushima, T. Kiss, K. Kobayashi, S. Shin, K.

Moriguchi, A. Shintani, H. Fukuoka, and S. Yamanaka, *Phys. Rev. B* **64**, 172504 (2001).
¹⁸B. Williams, *Compton Scattering* (McGraw-Hill, London, 1977).
¹⁹N. Shiotani, *Jpn. J. Appl. Phys., Part 1* **38**, 18 (1999).
²⁰A. Bansil, *Z. Naturforsch., A: Phys. Sci.* **48**, 165 (1993).
²¹P. Eisenberger, *Phys. Rev. A* **5**, 628 (1972).
²²A. Ammer, C. Cros, M. Pouchard, J. M. Bassat, G. Villerneuve, M. Duttine, M. Menetrier, and E. Reny, *Solid State Sci.* **5**, 393 (2004).
²³N. Hiraoka, M. Ito, T. Ohata, M. Mizumaki, Y. Sakurai, and N. Sakai, *J. Synchrotron Radiat.* **8**, 26 (2001).
²⁴M. Ito and Y. Sakurai, *Synchrotron Radiation Instrumentation: Eighth International Conference* (AIP, NY, 2004), pp. 901-904.
²⁵Y. Sakurai and M. Ito, *J. Phys. Chem. Solids* **65**, 2061 (2004).
²⁶F. Biggs, L. B. Mendelsohn, and J. B. Mann, *At. Data Nucl. Data Tables* **16**, 201 (1975).
²⁷N. Sakai, *J. Phys. Soc. Jpn.* **56**, 2477 (1987).
²⁸T. Takeda and J. Kübler, *J. Phys. F: Met. Phys.* **9**, 661 (1979).
²⁹H. J. F. Jansen and A. J. Freeman, *Phys. Rev. B* **30**, 561 (1984).
³⁰S. H. Vosko, L. Wilk, and M. Nusair, *Can. J. Phys.* **58**, 1200 (1980).
³¹C. A. Coulson, *Proc. Cambridge Philos. Soc.* **37**, 55 (1941).
³²C. A. Coulson and W. E. Duncanson, *Proc. Cambridge Philos. Soc.* **67**, 55 (1941).
³³W. Weyrich, P. Pattison, and B. G. Williams, *Chem. Phys.* **41**, 271 (1979).
³⁴G. B. Adams, M. O'Keeffe, A. A. Demkov, O. F. Sankey, and Y.-M. Huang, *Phys. Rev. B* **49**, 8048 (1994).
³⁵M. E. Preil, J. E. Fischer, S. B. DiCenzo, and G. K. Wertheim, *Phys. Rev. B* **30**, 3536 (1984).